Jpn. J. Appl. Phys. Vol. 42 (2003) pp. 1628–1632
Part 1, No. 4A, April 2003

Fabrication of Surface-Stabilized Ferroelectric Liquid Crystal Display with Stripe-Shaped Domain Structure

Ruibo LU, Shin-Tson WU and Keshu XU[1]

School of Optics/Center for Research and Education in Optics and Lasers (CREOL), University of Central Florida, Orlando, FL 32816, U.S.A.
[1]*Department of Optics and Engineering, Fudan University, Shanghai 200433, China*

(Received October 4, 2002; accepted for publication December 2, 2002)

A uniform stripe-shaped domain (SSD) structure was obtained in the initial ferroelectric liquid crystal (FLC) alignment by rubbing the polyimide films doped with silicon naphthalocyanine. Such a surface-stabilized FLC cell exhibits a high contrast ratio and excellent bistability. Atomic force microscope images and pretilt angle measurement results demonstrated that the rubbing-induced polishing and flattening on the doped polyimide alignment films and the ordered arrangement of polymer aggregations are the main factors determining the formation of SSD structures. Using such alignment technique, a 64×80 FLC display device was assembled. The display panel shows 80 μs response time and >90% bistable memory capability. The device stability is also improved due to the existence of the SSD structure. [DOI: 10.1143/JJAP.42.1628]

KEYWORDS: ferroelectric liquid crystal, stripe-shaped domain, alignment, atomic force microscope

1. Introduction

Surface-stabilized ferroelectric liquid crystal (SSFLC) exhibits a fast response, wide view angle and bistable memory capability and has been considered for light shutter and display applications.[1)] However, technical issues on the zig-zag defects, mechanical stability and DC voltage balance still hinder SSFLC from widespread applications. The zig-zag defects tend to deteriorate the electro-optic (EO) properties of the devices, while the mechanical and shock-sensitive FLC alignment and residual DC voltage would cause concerns for long-term stability.

Some methods have been proposed to eliminate the zig-zag defects in SSFLC cells, which include the use of special polymer films[2)] and the glancing-angle evaporated SiO_2 films[3)] for providing the unidirectional-bent SmC* layers, the AC voltage stabilization for the undulation of FLC configuration[4)] and the adoption of FLC materials with naphthalene rings to produce book-shelf structure.[5)] Zig-zag free C1 and C2 states have also been obtained using the photoalignment technique[6)] and PI-RN1199 alignment films.[7)]

As a special case of the zig-zag defects, the stripe-shaped domain (SSD) structure can be obtained if an external electric field is applied in the SmA or SmC* phase during the temperature cooling process.[8,9)] In comparison with other FLC textures, the SSD structure helps to maintain LC alignment stability while exhibiting good bistability. The SSD structure can also be formed in the initial FLC alignment by doping phthalocyanine and naphthalocyanine compounds into the aligning agents,[10,11)] where the EO characteristics and stability of SSFLC cells can be improved simultaneously.

In this paper, we report a new naphthalocyanine compound for enhancing the FLC alignment. The compound exhibits a good chemical and thermal stability and a good solubility in the polymer precursor. It is a promising dopant candidate for obtaining uniform FLC alignment. The formation mechanism and the control of the SSD structure are discussed on the basis of getting the optimal dopant ratio for achieving good molecular alignment, EO characteristics and bistable memory capability. In addition, a 64×80 mini-FLC display (FLCD) with 1.2 inch diagonal was fabricated.

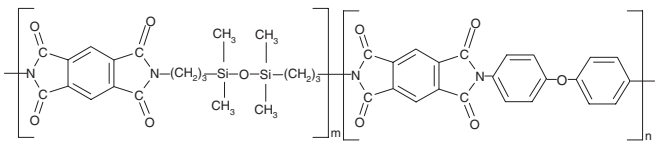

Fig. 1. The chemical structure of the polyimide compound used for alignment studies.

2. Experimental

The new dopant we developed is silicon naphthalocyanie, abbreviated as SiNc. It exhibits a good solubility in the polyamic acid solution and meltability with the thus imidized polymer films shown in Fig. 1. The doping concentration of SiNc in the polyamic acid solution ranges from 0.1% to 0.3% in weight. The solution was spun onto the indium-tin-oxide (ITO) substrates at 4,000 rpm rate and then baked at 200°C for 1 hr for the imidization to get the SiNc doped polyimide (PI) films. The resulting PI films were rubbed unidirectionally under a velvet-covered cylinder. Empty LC cells were fabricated with the substrate rubbing directions parallel to each other. The cell gap was controlled at 1.5–1.8 μm with the photolithographic polymer spacers. The FLC material CS-1024 (Chisso Co., Japan) was injected into the empty LC cell by capillary flow at a temperature above the LC clearing point and then cooled down to the room temperature slowly. The CS-1024 FLC mixture has the following phase transition sequence: Crystal (−12°C) → SmC* (62°C) → SmA (82°C) → N* (90°C) → Isotropic.

An anti-parallel cell was assembled for the pretilt angle measurement in the nematic phase. A cell with 27 μm gap was filled with nematic liquid crystal mixture ZLI-3417-006 (Merck, Germany) under vacuum. The crystal rotation method which has precision up to 0.01° (DMS-501, Germany) was used for measuring the pretilt angle.

The microscopic textures of the SSFLC cells were observed using a polarizing microscope. The EO properties of the SSFLC cells were measured between the crossed polarizers using a He–Ne laser ($\lambda = 632.8$ nm). The light transmittance was detected by a photomultiplier and recor-

ded in a dual-channel digital oscilloscope. The contrast ratio was measured under the application of a ±20 V, 10 Hz rectangular voltage. The rise and decay times are defined as the transmittance changes from 10% to 90% and vise versa. The bistability (or the memory capability) was measured using a 1 ms bipolar pulse with a period of 20 ms. An atomic force microscope (AFM, Nanoscope III, Digital Instrument, USA) was used to characterize the surface morphology of the rubbed PI films. The AFM scan was carried out on the ITO substrates under the constant force mode in air at 20°C. The force between the sharp Si_3N_4 tip and the substrate was on the order of 10 nN.

3. Results and Discussions

3.1 Polarizing microscope textures

Figure 2 shows the typical cross-polarizer microscopic textures of the SSFLC cells using the rubbed PI alignment films containing 0.2% SiNc. The applied rubbing forces can be controlled at the precision of ±2 gram-force (gf) and are categorized into weak (∼5 gf), medium (∼10 gf) and strong (15–20 gf) levels according to the rubbing strength. From Fig. 2(a), the focal-conic and half-splayed ferroelectric domain textures are apparent in the weak rubbing condition. These defects caused inhomogeneous alignment although the oriented part of FLC directors have tendency to align along the rubbing direction. For the medium rubbing strength as shown in Fig. 2(b), the alignment uniformity was greatly improved and fewer focal-conic defects observed. Some orderly aligned narrow and long stripe-shaped multi-domains along the rubbing direction are observed. The average width is about 7.5 μm. With the increased rubbing strength, the corresponding SSD structure becomes narrower and denser as shown in Fig. 2(c). Under the strong rubbing condition, the width of the SSD structure is reduced to ∼2 μm, which is comparable to the cell gap.

With the increased rubbing strength, the alignment of FLC directors changes from uneven to ordered state and the width of the multi-domain structure shrinks. As a result, the alignment defects are reduced and alignment uniformity improved. This indicates that the surface morphology of the rubbed alignment layers plays an important role in the FLC alignment.

3.2 AFM images

Figures 3(a), (b) and (c) show the AFM surface morphologies of the SiNc/PI films under weak, medium and strong rubbing strengths, respectively. The polymer grooves are evident on the weakly rubbed films and the width ranges from tens to several hundreds of nanometers. For the medium rubbing strength, the groove density increases, the average width is 21 nm and the groove height is lowered. This demonstrates that the rubbing process has the flattening and polishing effect on the PI films. The same phenomenon is amplified on the strongly rubbed PI surface, where not only the previous irregular protrusions on the PI

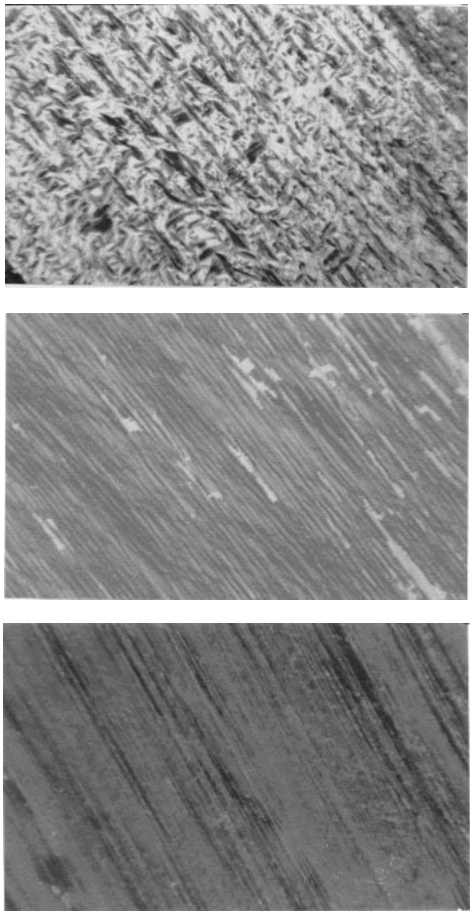

Fig. 2. The SSD structures in SiNc doped SSFLC cells observed under the polarizing microscope. (a): weak, (b): medium and (c): strong rubbing.

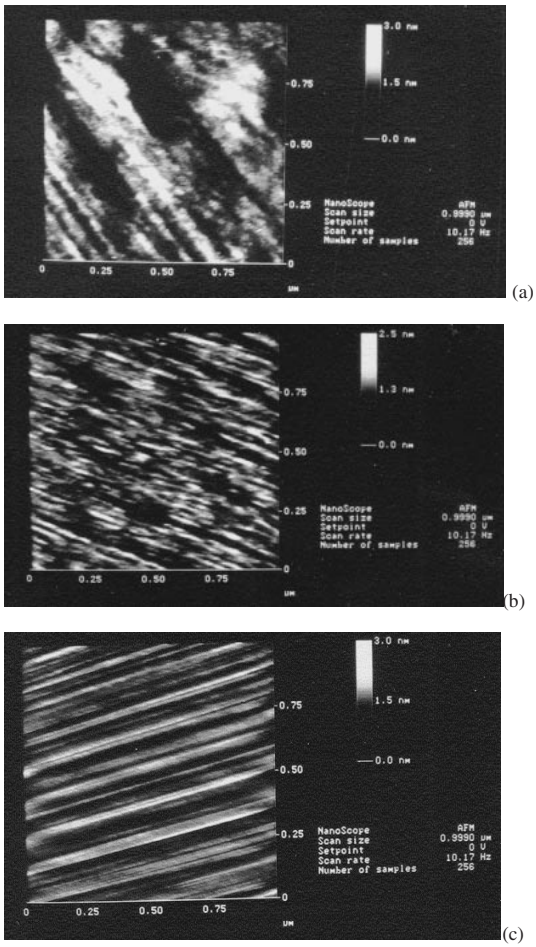

Fig. 3. AFM images of SiNc doped aligning films rubbed under different rubbing strengths. (a): weak, (b): medium and (c): strong rubbing.

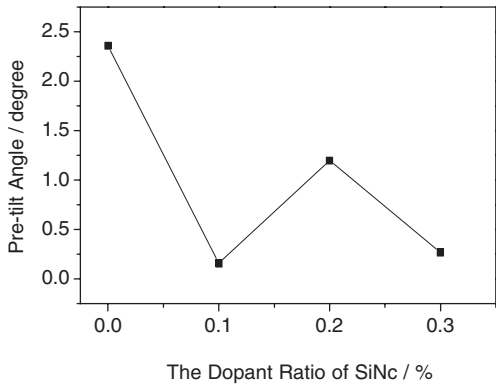

Fig. 4. The relationship between the pretilt angle of the NLC cells and the SiNc dopant concentration. LC: Merck ZLI-3417-006.

surface disappeared but also the corresponding groove structure became well-arranged and separated by ~14 nm between the neighboring grooves. In addition, a more detailed polymer aggregated orientation is observed on the groove structure. Based on the above-mentioned FLC alignment, it can be regarded that the formation of the SSD structure is closely connected to the rubbing process. The polished and flattened alignment layer is beneficial to the formation of the narrower SSD structure in the SiNc/PI alignment film.

3.3 Pretilt angle measurement

Figure 4 plots the induced pretilt angle of the NLC cells as a function of SiNc doping concentration in PI films for the case of strong rubbing condition. For the undoped LC cell, its pre-tilt angle is 2.36°. As the SiNc concentration increases from 0.1, 0.2 to 0.3%, the pretilt angle decreases to 0.16°, 1.20° to 0.27°, respectively.

After doping the SiNc to polyimide, the interaction between the LC molecules and the aligning agents is strengthened. This makes the LCs more likely to lie flat on the film surfaces. The phenomenon can be explained from the special chemical structure of the doped SiNc molecules. The naphthalocyanine rings are brought into the PI system through the doping enhanced interaction with the LC molecules. As a result, the modified alignment films have a stronger anchoring force. As for why there is a relatively high pretilt angle at 0.2% dopant ratio, it is speculated due to a certain screening effect between the distribution of SiNc and PI which weakens their anchoring action to the LC molecules. This argument is supported by our other experimental observations. The LC cells prepared by the same amount of SiNc doping while treated under different rubbing strengths show nearly the same pretilt angles, even though the AFM images revealed a notable difference in their surface morphologies.

3.4 EO characteristics of SSFLC cells

Figures 5(a), (b) and (c) depict the SiNc doping concentration effects on the bistable memory capability and contrast ratio of the SSFLC cells treated with weak, medium and strong rubbing strength, respectively. Overall speaking, as the rubbing strength increases, the bistable memory capability and contrast ratio both increase. Within each rubbing strength category, the SSFLC cells with the

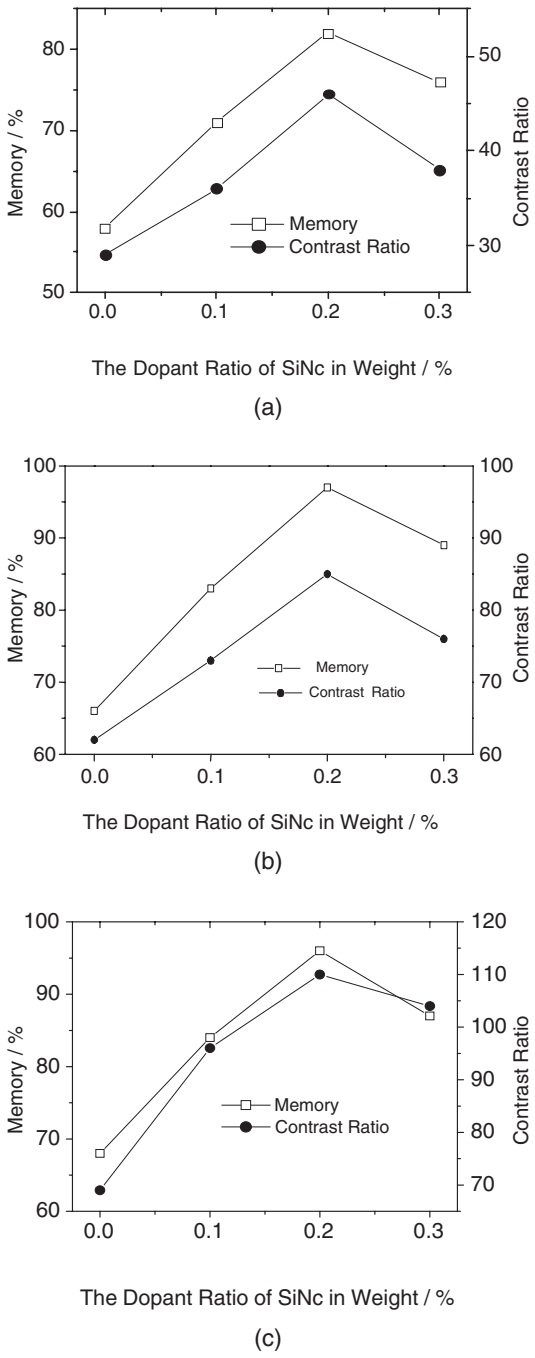

Fig. 5. The memory capability and contrast ratio of the SSFLC cells at different dopant ratios. (a): weak, (b): medium and (c): strong rubbing.

SiNc doped PI alignment layers clearly show improvement in both bistability and contrast ratio in comparison with that of the undoped SSFLC cell. From Figs. 5(a), (b) and (c), the best EO properties seem to all occur at 0.2% SiNc dopant ratio. For the weak, medium and strong rubbing strength, the best bistability reaches 82, 97 and 97%, and contrast ratio 46 : 1, 86 : 1, 110 : 1, respectively. The high contrast ratio observed in the strong rubbing cell is attributed to the existence of the denser SSD structure which keeps a darker initial alignment. As the external voltage is applied, the layered SSD structure is changed from inter-hinged chevron to bookshelf or quasi-bookshelf structure. Thus, a maximum light transmission is achieved and a higher contrast ratio is obtained.[9,12)]

3.5 Rubbing process effect on FLC alignment

In a previous report, Geary *et al.*[13] suggested that the homogeneous alignment of nematic and smectic LCs can be achieved if the aligning polymer has orientation and crystalline nature. Hartmann *et al.*[14] regarded that there were two orientation directions from the polymer layers in the liquid crystal alignment, where the in-plane orientation was caused by the stretching of the polymer chains along the rubbing direction and the out-of-plane orientation was controlled by the flattening of the polymer chains onto the rubbed surfaces. And Kikuchi *et al.*[15] also found that both the degree of order and mechanical properties of the aligning polymer films played important roles in the alignment of smectics.

According to the above experiments, the initial alignment of FLC is mainly determined by the rubbing process which, in turn, affects the EO characteristics of the corresponding devices. The weak rubbing strength brings out the nonuniform FLC alignment with lots of focal-conic defects. As the rubbing strength increases, the irregular defects are suppressed and the uniform and wide SSD structures appear. At strong rubbing condition, the SSD structures become narrower and denser. Consequently, the EO properties of the SSFLC cells, especially the contrast ratio, are improved as the rubbing strength increases.

Under the weak rubbing condition, the polymer surface is just partly oriented along the rubbing direction as shown in Fig. 3(a). Under this circumstance, a uniform alignment for nematic liquid crystal could still be obtained macroscopically. Nevertheless, FLC is harder to align. Due to the irregularity of the polyimide surface, it is difficult to align smectic layers without defects.

The increased rubbing strength helps to polish and flatten the alignment films resulting in denser groove structures. From Fig. 3(b), the surface morphology of the rubbed polymer films starts to exhibit order. When the LCs enter the SmA phase from the nematic phase, the smectic layers would not remain completely perpendicular to the aligning surface due to the out-of-plane tendency. The SmA layers would tilt corresponding to the substrate surface normal during the SmA $\rightarrow$ SmC* phase transition. Although the number of tilted layers in the SmA can be supposedly controlled by the out-of-plane orientation, the chevron structure with the opposite bending directions takes place in the following SmC* phase due to the random appearance of the SmA layers. As a result, the zig-zag defects occur.

With the further increase in rubbing strength, the microgrooves formed by the ordered polymer chains exhibit a stronger anisotropic force to lower the out-of-plane degree of LCs and diminish the SmA layers that are not perpendicular to the substrate surface. Consequently, the defects in the SmC* phase become less and the corresponding SSD structure becomes narrower. This observation is consistent with the theoretical prediction[16] when the width of the SSD structure is comparable to the cell gap. Therefore, it can be concluded that the polishing and flattening onto the doped aligning PI films through the rubbing process and the ordered arrangement of the polymer aggregations are the main factors that determine the SSD structure formation.

4. 64 × 80 mini-FLCD

Based on the alignment technology described above, we have fabricated a mini FLC display panel with 64 × 80 resolution elements. The panel structure and its electro-optic characteristics are discussed in the following.

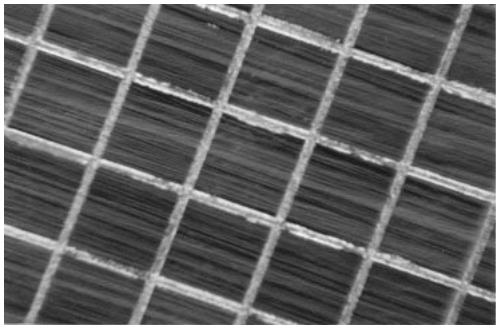

Fig. 6. The stripe-shaped domain structure of a 64 × 80 FLCD under the polarizing microscope. Magnification ratio: 200 X. The SiNc dopant ratio: 0.2 wt%.

4.1 Polarized microscope graph

A 64 × 80 mini-FLCD device with uniform alignment area of 30 mm × 30 mm and an effective diagonal of 30.48 mm was fabricated using the SiNc/PI alignment films. The pixel size is 270 μm × 270 μm with 30 μm gap between the neighboring pixels. Figure 6 shows the photograph of the FLC display device. As observed through the polarizing microscope, the FLCs exhibit SSD structure in the individual pixels. The average width of the SSD structure is ~5 μm.

4.2 EO characteristics of FLCD

The measured rise and decay time of the 64 × 80 FLCD panel is 80 μs, respectively, and contrast ratio is 55 : 1. Figure 7(a) shows the bistability of the SSFLC device using the 0.2% SiNc doped PI alignment layers. The bistability is higher than 90%. In contrast, the SSFLC with undoped alignment layers as shown in Fig. 7(b) generally has less than 60% bistability.

Similar to our previously fabricated 64 × 64 spatial light modulator using SnPc as dopant,[12] the 64 × 80 FLCD using SiNc/PI alignment layers retains the SSD structure without degradation. Moreover, it shows stable EO properties after long term storage or operation. On the other hand, the nondoped device would show a certain degeneracy of the SmC* structure which can not be easily restored even under AC stabilization. Therefore, the SiNc doped PI alignment layers have better stability due to the formation of SSD structure. In the mean time, a relatively large uniform FLC alignment area can be achieved. These two aspects are valuable from the viewpoint of practical applications. The improved alignment agent is useful for developing large size and high resolution FLCD devices.

5. Conclusion

The organic compound SiNc with a better solubility and meltability was chosen as the dopant in the rubbed PI aligning films for SSFLC alignment. Uniform SSD structure is obtained without the application of external electric field in the initial alignment, and the width and uniformity are controlled by the rubbing process. The corresponding SSFLC cells show a high contrast ratio and excellent memory capability. The optimal doping ratio and rubbing

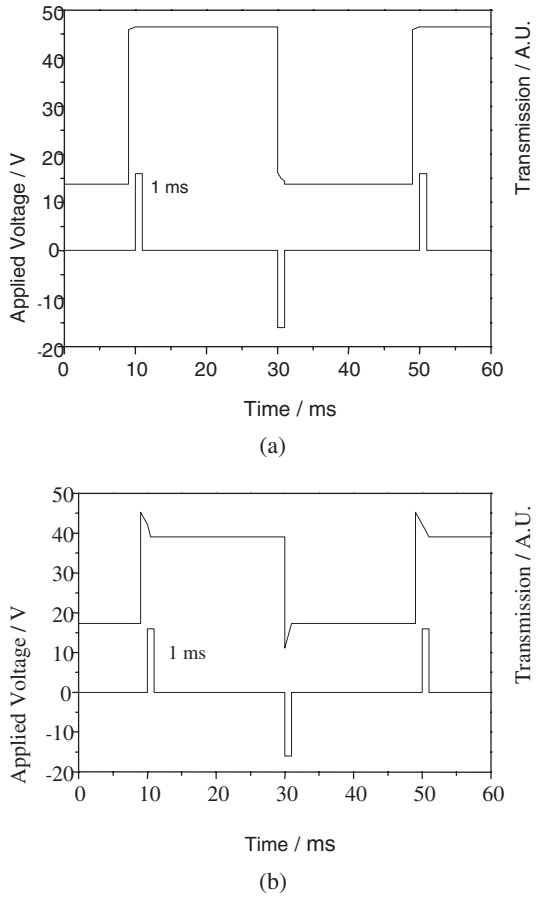

Fig. 7. Optical response of the SiNc doped (a) (at 0.2% dopant ratio) and un-doped (b) rubbing PI films aligned 64×80 FLCD. The applied voltage is ± 10 V/μm under 1 ms bipolar pulses with 20 ms periodicity.

condition were pursued and the role of the rubbing induced surface morphology in the SSD structure formation was investigated through AFM scanning and pretilt angle measurement. It is regarded that the polishing and flattening onto the doped aligning PI films through the rubbing process and the orderly arrangement of the polymer aggregations are the main factors affecting SSD structures.

A SSD type 64×80 mini-FLCD device with uniform alignment area of 30 mm $\times$ 30 mm and an effective diagonal of 1.2 inch was assembled using the SiNc doped PI films as the alignment layers. The display has 80 μs rise and decay time, 55 : 1 contrast ratio and $>90\%$ bistable memory capability. The device stability has also been improved due to the existence of the SSD structure. These properties will be valuable to the practical device application and for the further development of larger area and higher definition FLCD devices.

The UCF group is indebted to the financial support of AFOSR under contract number F49620-01-1-0377.

1) N. A. Clark and S. T. Lagerwall: Appl. Phys. Lett. **36** (1980) 899.
2) N. Yamamoto, Y. Yamada, K. Mori, H. Orihara and Y. Ishibashi: Jpn. J. Appl. Phys. **28** (1989) 524.
3) S. Kaho, T. Masumi, S. Tahata, M. Mizunuma and S. Miyake: Jpn. J. Appl. Phys. **30** (1991) 87.
4) S. Bawa, K. Saxena and S. Chandra: Jpn. J. Appl. Phys. **28** (1989) 662.
5) A. Mochizauki and S. Kobayashi: Mol. Cryst. Liq. Cryst. **243** (1994) 77.
6) R. Kurihara, H. Furue, T. Takahashi and S. Kobayashi: Proc. Soc. Inf. Disp. **31** (2000) 807.
7) H. Furue, Y. Iimura, Y. Miyamoto, H. Endoh, H. Fukuro and S. Kobayashi: Jpn. J. Appl. Phys. **37** (1998) 3417.
8) J. Pavel and M. Glogarova: Liq. Cryst. **9** (1991) 87.
9) R. Shao, P. Willis and N. Clark: Ferroelectrics **121** (1991) 127.
10) R. Lu, K. Xu, S. Zhang, Y. Le, H. Deng, N. Gu and Z. Lu: Mol. Cryst. Liq. Cryst. **333** (1999) 35.
11) R. Lu, K. Xu and Z. Lu: Liq. Cryst. **26** (1999) 553.
12) R. Lu, K. Xu, S. Zhang, X. Gu and Z. Xing: Acta Phys. Sin. (Overseas Edition) **8** (1999) 9.
13) J. Geary, J. Goodby, A. Kemtz and J. Patel: J. Appl. Phys. **62** (1987) 4100.
14) W. Hartmann and A. Luyckx-Smolders: J. Appl. Phys. **67** (1990) 1253.
15) H. Kikuchi, J. Logan and D. Yooh: J. Appl. Phys. **79** (1996) 6811.
16) Y. Asao and T. Uchida: Jpn. J. Appl. Phys. **32** (1993) L604.